energies

MDPI

Article

Numerical Simulation Research on Combustion and Emission Characteristics of Diesel/Ammonia Dual-Fuel Low-Speed Marine Engine

Qinran Wu [1], Xingyu Liang [1,*], Zhijie Zhu [1], Lei Cui [2] and Teng Liu [2]

[1] State Key Laboratory of Engines, Tianjin University, Tianjin 300072, China; wuqinran@tju.edu.cn (Q.W.)
[2] China Ship Power Institute Co., Ltd., Shanghai 201206, China
* Correspondence: lxy@tju.edu.cn

Abstract: Amid increasingly stringent global environmental regulations, marine engines are undergoing an essential transition from conventional fossil fuels to alternative fuels to meet escalating regulatory requirements. This study evaluates the effects of injection pressure, the timing of ammonia injection, and the pre-injection of ammonia on combustion and emissions, aiming to identify optimal operational parameters for low-speed marine engines. A three-dimensional model of a large-bore, low-speed marine engine in a high-pressure diffusion mode was developed based on computational fluid dynamics (CFD). Simulations were conducted under 25%, 50%, 75% and 100% loads with a high ammonia energy substitution rate of 95%. The results indicate that, compared to traditional pure diesel operation, adjusting the injection pressure and the ammonia injection timing, along with employing appropriate pre-injection strategies, significantly enhances in-cylinder pressure and temperature, improves thermal efficiency, and reduces specific fuel consumption. Additionally, the dual-fuel strategy using diesel and ammonia effectively reduces nitrogen oxide emissions by up to 37.5% and carbon dioxide emissions by 93.7%.

Keywords: marine engines; ammonia fuel; dual-fuel engine; emissions

check for updates

Citation: Wu, Q.; Liang, X.; Zhu, Z.; Cui, L.; Liu, T. Numerical Simulation Research on Combustion and Emission Characteristics of Diesel/Ammonia Dual-Fuel Low-Speed Marine Engine. *Energies* **2024**, *17*, 2960. https://doi.org/10.3390/en17122960

Academic Editor: Leszek Chybowski

Received: 24 April 2024
Revised: 29 May 2024
Accepted: 31 May 2024
Published: 16 June 2024

Copyright: © 2024 by the authors. Licensee MDPI, Basel, Switzerland. This article is an open access article distributed under the terms and conditions of the Creative Commons Attribution (CC BY) license (https://creativecommons.org/licenses/by/4.0/).

1. Introduction

The escalation of human activities has brought climate variability to the forefront of global concern [1]. In response, concerted efforts are underway to mitigate the impact on the climate by transitioning from a fossil-fuel-dominated society, characterized by high carbon emissions, to one propelled by renewable energy sources with reduced or zero carbon emissions. The maritime industry, a cornerstone of the global economy, is a significant contributor to annual greenhouse gas emissions [2]. Recent years have witnessed maritime activities contributing between 2% and 3% of total global emissions, primarily consisting of CO_2 emissions [3], with a discernible upward trend. In light of this, the International Maritime Organization (IMO) has issued the "Initial Strategy for Greenhouse Gas Emission Reduction from Ships" [4], outlining crucial emission reduction milestones: implementing specific measures to reduce greenhouse gas emissions from ships by 2023, achieving a minimum of a 40% reduction in emissions by 2030 compared to 2008 levels, and targeting a minimum of a 70% reduction by 2050, ultimately aiming to eliminate ship greenhouse gas emissions by the century's end [5]. Realizing zero carbon emissions from ships necessitates an energy transition for maritime vessels. Currently, primary maritime fuels, such as heavy oil and diesel, yield substantial quantities of CO_2, sulfur oxides, nitrogen oxides, and other pollutants, posing significant environmental and human health hazards [6]. Thus, identifying low-carbon or zero-carbon alternative fuels is pivotal for a maritime energy transition. Among the array of alternative fuels, ammonia stands out as one of the most promising zero-carbon options, primarily due to its capacity for generating water and nitrogen upon complete combustion [7].

However, ammonia as a fuel is not without its drawbacks. Firstly, its combustion rate, flame speed, and stable combustion limits are relatively low, resulting in diminished combustion efficiency [8]. Secondly, ammonia requires high ignition energy and high temperatures to start burning, thereby encountering challenges with ignition. Additionally, due to its high latent heat of vaporization [9], the injection of ammonia into the cylinder may significantly lower internal cylinder temperatures, thus affecting combustion efficiency [10]. Lastly, the combustion of ammonia fuel unavoidably generates emissions of unburnt ammonia and nitrogen oxides, with unburnt ammonia emissions being known for their irritant, toxic, and corrosive properties [11]. Furthermore, the greenhouse effect of nitrous oxide emissions substantially exceeds that of carbon dioxide, highlighting an issue in need of resolution [12]. Consequently, engines commonly employ a dual-fuel mode, utilizing diesel for ammonia combustion initiation, with optimization efforts focused on this mode [13].

In recent years, numerous scholars have conducted extensive research on the combustion and emissions of ammonia-fueled engines. Several studies [14–18] have been carried out on the effects of different ammonia energy replacement rates, injection strategies and combustion patterns on engine performance, and some scholars [19–22] have also investigated the emissions of the engine, including NO_X, N_2O and unburned NH_3.

Currently, research on diesel/ammonia dual-fuel marine engines primarily focuses on medium-speed and high-speed engines, as well as small-bore engines. To date, there has been no reported research on large-bore, low-speed engines. Therefore, the focus of this study is on large-bore, low-speed marine engines.

This study aims to numerically investigate the effects of various injection parameters on the combustion and emission characteristics of a large-bore, low-speed marine engine operating in a high-pressure diffusion combustion mode, using a computational fluid dynamics (CFD) approach. The optimized parameters in this study, i.e., the injection pressure, the ammonia injection timing and the pre-injection strategy, are intended to establish the optimum combustion strategy for the implementation of a diesel/ammonia dual-fuel mode in a large-bore low-speed marine engine.

2. Methodology

2.1. Engine Parameters

This research focuses on a two-stroke marine low-speed engine with a cylinder diameter of 520 mm. The 3D model of the original engine is shown in Figure 1. The original engine has three fuel injectors, which are all located at the top of the cylinder. Other main parameters are shown in Table 1.

Figure 1. Engine geometric model.

Table 1. Basic size parameters of the original engine.

Basic Parameters	Value
Number of strokes	2
Fuel	diesel
Cylinder diameter (mm)	520
Stroke length (mm)	2658
Geometric compression ratio	21.8
Rotating speed (rpm)	103
Maximum pressure (bar)	250

2.2. Simulation Model Setup

The physical models used in the three-dimensional computation are detailed in Table 2, and this model is constructed in CONVERGE. The adopted chemical reaction kinetics mechanism is the diesel/ammonia mixed chemical reaction kinetics mechanism (97 species, 498 reactions) [23]. This mechanism has been experimentally validated and is applicable to the experimental conditions of this study. The initial conditions and some temperature and pressure boundary conditions in the established simulation model are based on previous experiments and simulations, as listed in Table 3. High-pressure diffusion combustion is employed, and the dual-fuel mode is achieved by installing three ammonia injectors based on the original engine's three fuel injectors. In dual-fuel mode, the original three fuel nozzles are used for diesel injection, with diameters of 1.075 mm, 1.275 mm, 1.250 mm, 1.150 mm and 1.000 mm, respectively, and three ammonia injectors are arranged next to the fuel injector on the original basis respectively, and the injection direction is at an angle of 60° with the diesel injector as shown in Figure 2.

Table 2. Calculation submodels.

Calculation Submodel	Type
Turbulence model	RNG k-ε model
Spray breakup model	KH-RT model
Evaporation model	Frossling model
Droplet collision	NTC model
NO_X emission model	Y. Zeldovich model
Soot emission model	Hiroyasu-soot model
Combustion model	SAGE model
Drop/wall interaction	Wall film
Wall heat transferring model	O'Rourke and Amsden
Mechanisms of chemical reaction kinetics	C_7H_{14}/NH_3 [23]

Table 3. Intake and exhaust parameters and initial condition settings for the model.

Parameters	Value	Units
Exhaust valve opening time (EVO)	113	°CA
Exhaust valve closing time (EVC)	298	°CA
Initial cylinder pressure (relative pressure)	11.172	bar
Initial in-cylinder temperature (relative pressure)	1056.1	K
Boost pressure (relative pressure)	4.67	bar
Exhaust pressure (relative pressure)	4.30	bar

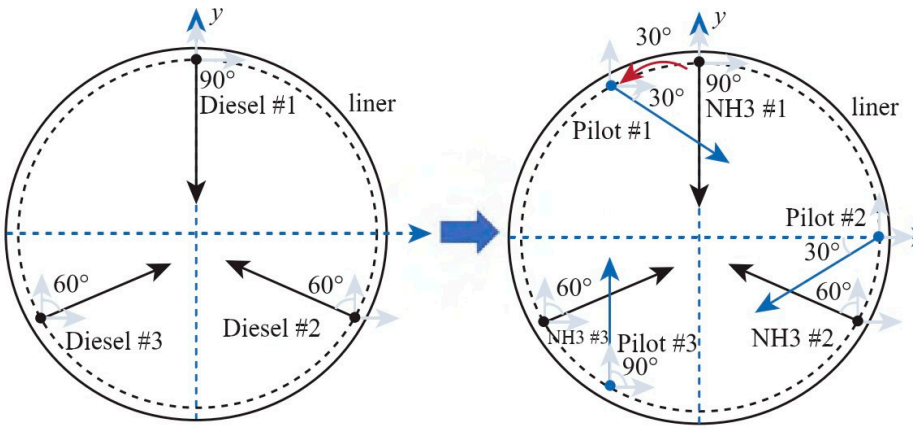

Figure 2. Injector arrangement.

2.3. Simulation Model Verification

Due to the considerable spatial dimensions of the marine low-speed engine, the mesh sensitivity analysis of the model constructed in this study has been validated in a previous study [24], and Table 4 lists the mesh strategies employed in the 3D model. The model was validated at 25%, 50%, 75% and 100% loads of the engine at an injection pressure of 700 bar, a diesel injection timing of 2.5 °CA BTDC. The results are shown in Figures 3 and 4. Figures 3 and 4 show the comparison between simulated and experimental data in terms of mean cylinder pressure and heat release rate. The findings affirm that the computational model utilized in the simulation can more precisely replicate the actual operating conditions of the engine. A comparison of simulated and experimental emissions at a 100% load used for the simulation is shown in Table 5.

Table 4. Grid strategy and grid size.

Grid Strategies	Region	Size/Level
Basic grid	overall	4 cm
Fixed embedding	cylinder injector	level 2 level 3
Adaptive mesh refinement	velocity-temperature	level 2

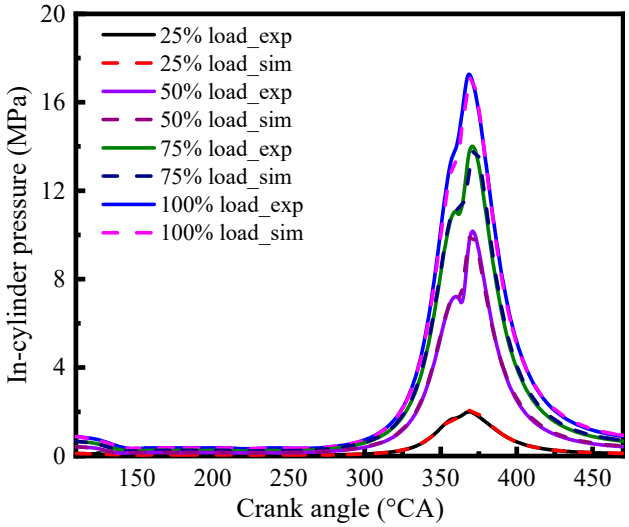

Figure 3. Comparison of average pressure in the cylinder at different loads in simulation and test [23].

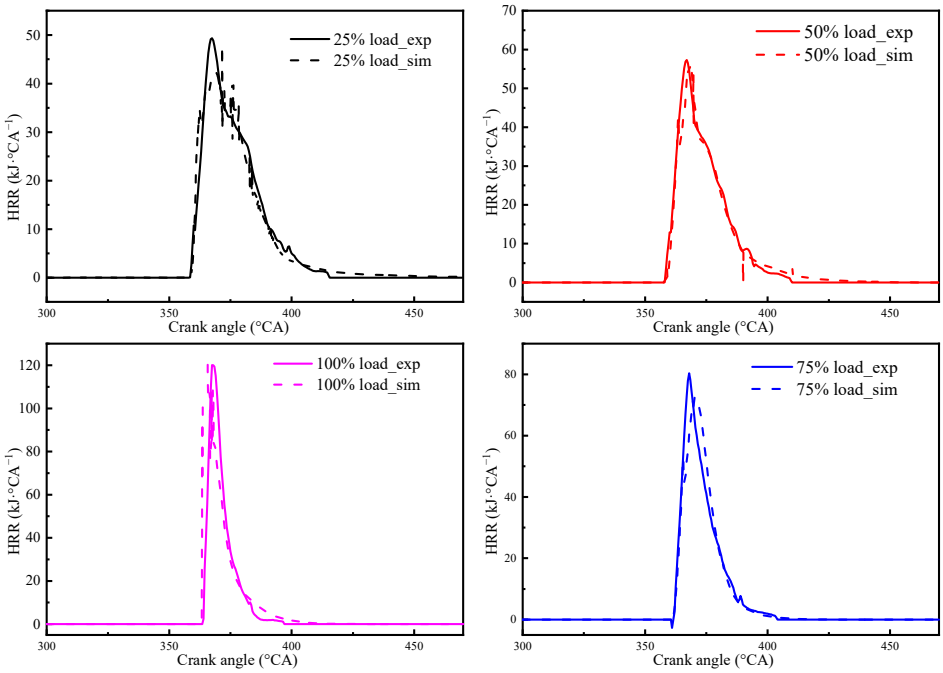

Figure 4. Comparison of HRR(heat release rate) in cylinder at different loads in simulation and test.

Table 5. Comparison of emissions at 100% load in simulation and test.

Emissions	Experiment/(g·(kW·h)$^{-1}$)	Simulation/(g·(kW·h)$^{-1}$)
NO_X	10.1	10.27
CO_2	34.2	33.9

2.4. Simulation Research Scheme

In this study, the main research includes the following parts: Firstly, this study investigates the effect of fuel injection pressure on a marine engine in a dual-fuel mode, where the injection pressure includes diesel and ammonia. The physico-chemical properties of the fuels are shown in Table 6. Secondly, this study investigates the effect of ammonia injection timing on the combustion and emissions of a marine engine. Then, in the study of the pre-injection, the changes in the combustion and emission characteristics of the engine were investigated for pre-injection ratios of 10% and 30% of the total ammonia injection, respectively. The numerical simulation study parameters used are shown in Table 7.

Table 6. Fuel properties [18].

Fuel Properties	Ammonia	Diesel
Research octane number	130	-
Boiling point (°C)	−33.4	180–360
Ignition point (°C)	800	220
Minimum ignition energy (MJ)	680	0.63
Low heating value (MJ/kg)	18.8	42.5
Laminar flame speed (cm/s)	10	33
Auto-ignition temperature (K)	930	527–558
Adiabatic flame temperature (K)	2073	2573

Table 7. Numerical simulation research conditions of dual-fuel combustion mode.

Case	Injection Pressure (bar)	Ammonia Pre-Injection Timing (°CA BTDC)	Diesel Injection Timing	Ammonia Injection Timing
1–4	500, 600, 700, 800	-	2.5 °CA BTDC	2.0 °CA BTDC
5–12	700	-	3, 2.5, 2, 1.5 °CA BTDC 0.5, 1, 1.5 °CA ATDC	2.5, 2.0, 1.5, 1 °CA BTDC 0, 0.5, 1 °CA ATDC
13–15	700	4.43, 10.8	2 °CA BTDC	1 °CA BTDC

3. Results

3.1. Effect of Diesel/Ammonia Injection Pressure on Combustion and Emission Characteristics of Low-Speed Engines

This section investigates the simulation study under the conditions of a 100% load, a 95% ammonia energy substitution rate, and injection timings of 2.5 °CA BTDC for diesel injection and 2 °CA BTDC for ammonia injection in the diesel/ammonia dual-fuel engine. Simulations are conducted at injection pressures of 500 bar, 600 bar, 700 bar and 800 bar (consistent for both diesel and ammonia).

Figure 5 illustrates the comparative analysis of the in-cylinder pressure and heat release rate, under different diesel/ammonia injection pressure conditions. It can be observed from the figures that as the injection pressure gradually increases, the in-cylinder pressure and heat release rate both show an increasing trend, and the peaks of the pressure and heat release rate are shifted earlier in the phase. This phenomenon is mainly attributed to the higher injection pressure promoting more effective fuel atomization, thereby accelerating the combustion rate.

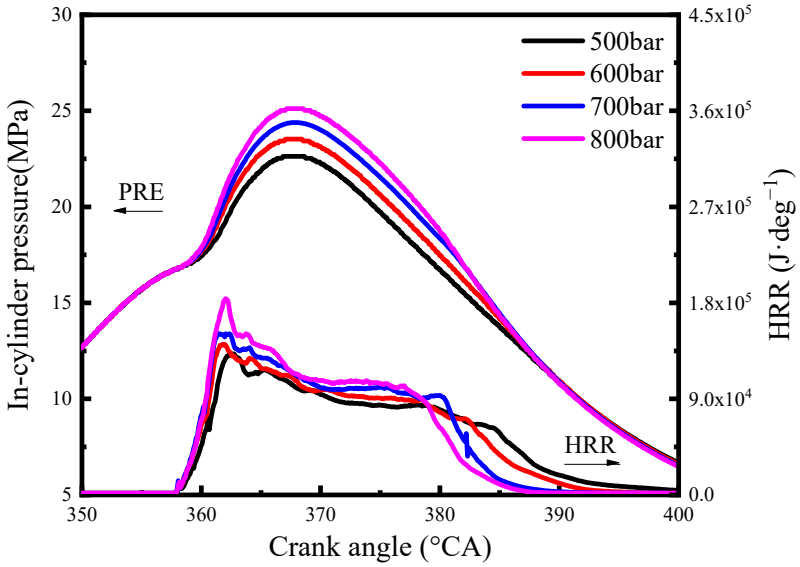

Figure 5. Effect of cylinder pressure across injection pressures.

The effects of injection pressure on the CA10 (the crankshaft angle at the beginning of combustion), the CA50 (the crankshaft angle at the middle of combustion), and the combustion duration are shown in Figure 6. Figure 6 illustrates the influence of injection pressure on the CA10 (the crank angle at 10% of heat release), the CA50 (the crank angle at 50% of heat release), and the combustion duration. The results indicate that the CA10 shows no significant variation with increasing injection pressure, while the CA50 and combustion duration exhibit an overall trend of initially decreasing followed by an increase. At an injection pressure of 500 bar, the CA10, CA50 and combustion duration reach their maximum values. This could be attributed to the lower injection pressure resulting in a slower fuel injection rate, requiring more time for fuel–air mixing to form a combustible

mixture, thereby prolonging the combustion duration. Moderate increases in injection pressure help shorten this process, improving combustion efficiency.

However, the results also demonstrate that the influence of injection pressure on the CA50 and combustion duration gradually diminishes with further pressure increases. At an injection pressure of 700 bar, the combustion process reaches its optimal state. However, when the injection pressure continues to rise to 800 bar, both the CA50 and combustion duration increase. This may be due to excessively high injection pressures accelerating the fuel injection rate, causing some fuel to adhere to the cylinder walls, deteriorating the combustion process, and resulting in a delay in the combustion phase and prolongation of the combustion duration.

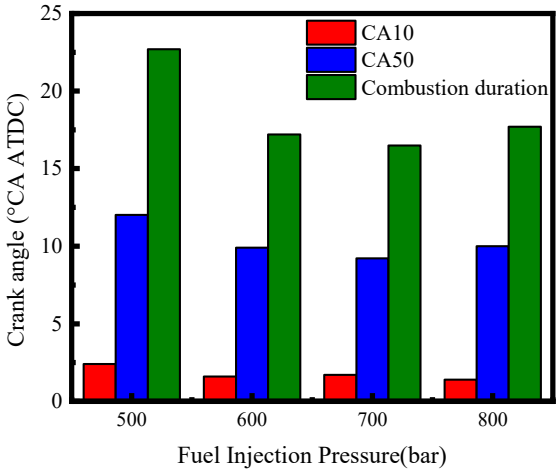

Figure 6. Comparison of CA10, CA50 and burn duration at different injection pressures.

Figure 7 compares the in-cylinder mixture distribution under different injection pressure conditions. At lower injection pressures (e.g., 500 bar), the mixture concentration distribution is more dispersed, indicating inadequate fuel–air mixing, and thus reducing the combustion efficiency. As the injection pressure increases to 600 bar and 700 bar, the mixture concentration distribution tends to be more uniform, indicating an improvement in fuel atomization at higher injection pressures, promoting the formation of a more homogeneous mixture. However, at the highest injection pressure (800 bar), some fuel may have adhered to the cylinder walls, potentially affecting mixture uniformity and combustion efficiency.

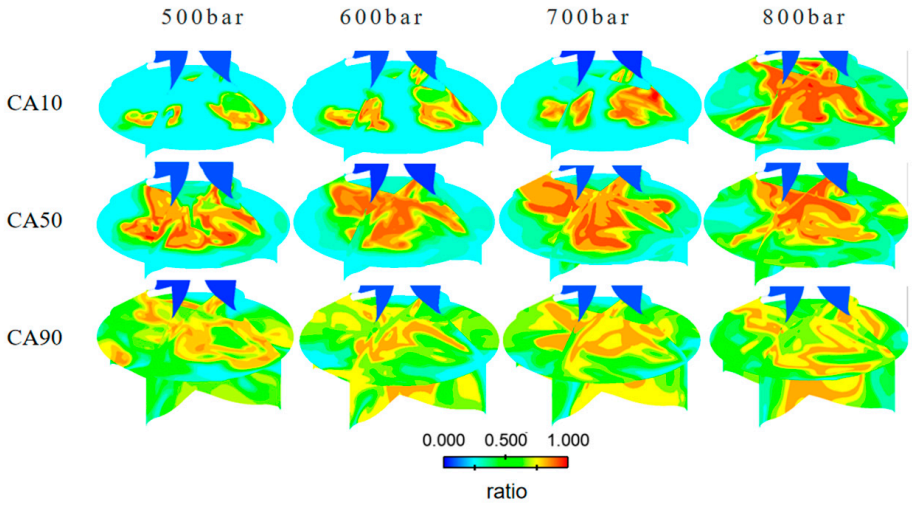

Figure 7. Comparison of in-cylinder mixture distribution at different injection pressures.

Figure 8 depicts variations in the average indicated mean effective pressure (IMEP), the thermal efficiency (ITE), and the indicated specific fuel consumption (ISFC) under different operating conditions, where the ISFC is calculated by converting the consumption of ammonia into the equivalent consumption of diesel fuel based on energy.

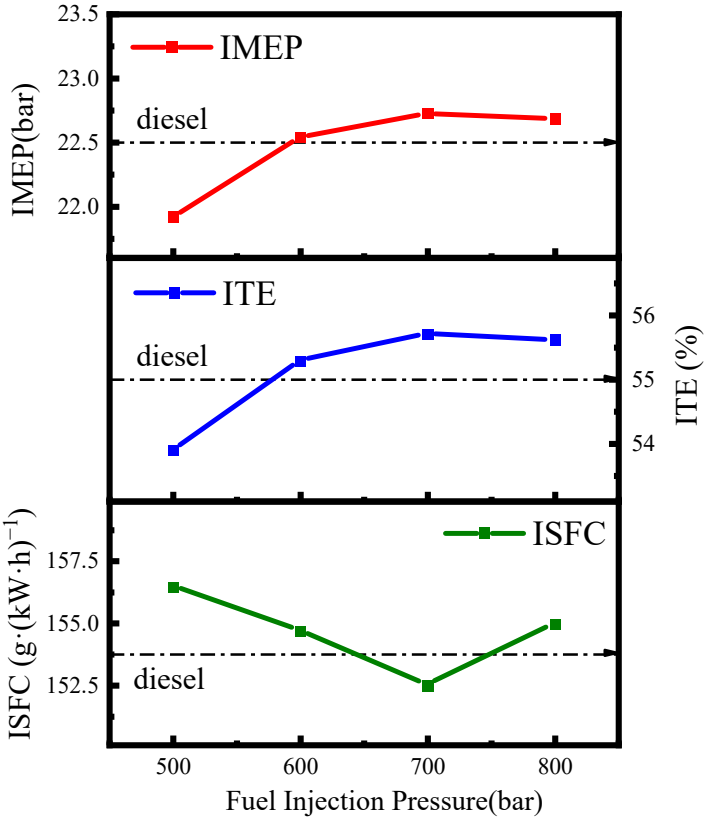

Figure 8. Comparison of IMEP, ITE and ISFC at different injection pressures.

However, the results in the figure also show that its effect on the CA50 and combustion duration diminishes with a further increase in injection pressure. The combustion process is optimized at an injection pressure of 700 bar. When the injection pressure continues to increase to 800 bar, the CA50 and combustion duration increase, which may be attributed to the high injection pressure accelerating the fuel injection velocity, resulting in part of the fuel adhering to the cylinder wall, deteriorating the combustion process, shifting the combustion phase backwards, and lengthening the combustion duration.

Figure 9 compares the distribution of in-cylinder temperatures under different injection pressure conditions. It can be observed that as the injection pressure increases, the area of high-temperature regions within the cylinder gradually expands, and the temperature distribution becomes more uniform. This is primarily attributed to the enhancement of the injection pressure, which improves the degree of fuel–air mixing, thereby promoting more effective combustion.

Figure 10 illustrates the variation trends of major emissions under different injection pressures. The results indicate a pattern of increasing and then decreasing NO_X emissions with increasing injection pressures. This trend may be closely related to the distribution of temperature within the combustion chamber and changes in local oxidation-reduction states. At lower injection pressures, inadequate atomization may lead to uneven fuel dispersion, resulting in an uneven distribution of temperatures and oxygen concentrations in localized areas, thus promoting NO_X formation. Conversely, as the injection pressure increases, improved fuel atomization and more uniform mixture formation leads to a more even combustion process, effectively reducing local high-temperature areas and decreasing NO_X generation.

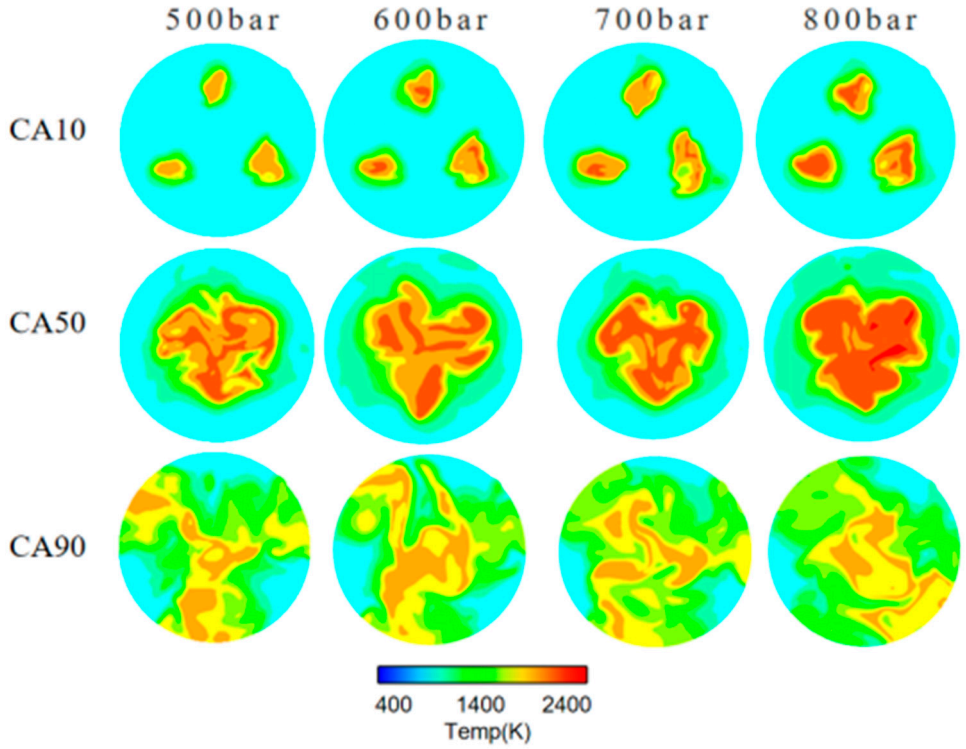

Figure 9. Temperature distribution in the engine cylinder under different injection pressures.

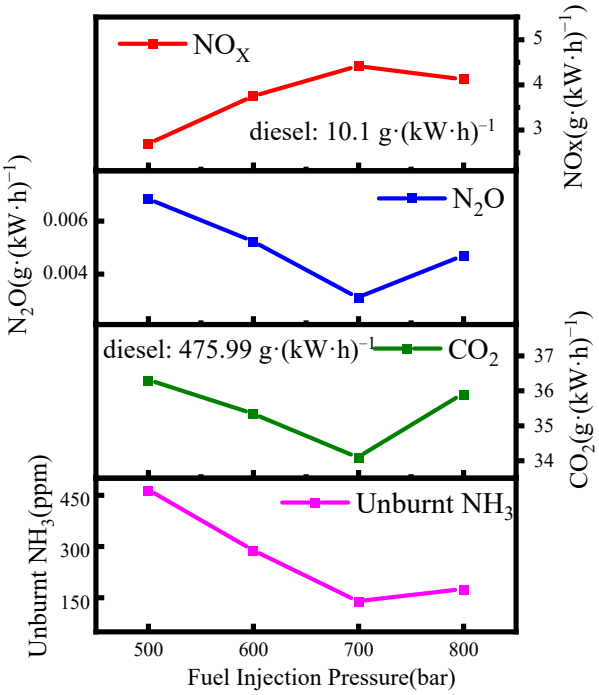

Figure 10. Comparison of NO_X, N_2O, CO_2 and unburnt NH_3 at different injection pressures.

For emissions of N_2O, CO_2, and unburnt NH_3, the emission trends show an initial decrease followed by an increase. This is mainly attributed to the initial improvement in fuel atomization quality with increasing injection pressures, which enhances fuel–air mixing and promotes more complete combustion, thereby reducing the generation of N_2O and CO_2 to some extent and decreasing unburnt NH_3 emissions. However, the increase in unburnt NH_3 emissions at 800 bar may be due to excessively fast injection speeds,

causing some ammonia gas to not fully mix with air before the exhaust process begins and participate in combustion reactions.

Figure 11 illustrates the distribution of cylinder NO_X under different injection pressure conditions. Analysis of the contour maps reveals that with the gradual increase in injection pressure, both the concentration and distribution area of NO_X initially show an increasing trend, followed by a leveling off for this trend. The area of high-concentration NO_X slightly expands, indicating that within a certain range, increasing the injection pressure improves combustion conditions and increases NO_X generation. However, further increasing the injection pressure to 800 bar does not significantly affect NO_X generation.

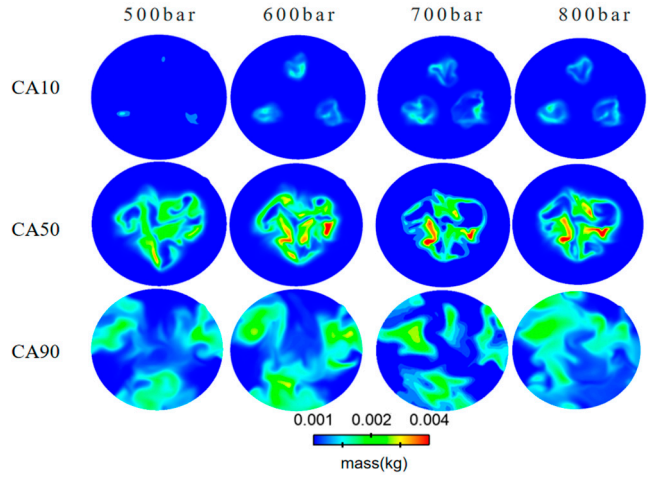

Figure 11. In-cylinder NO_X distribution at different injection pressures.

3.2. Effect of Diesel/Ammonia Injection Timings on Combustion and Emission Characteristics of Low-Speed Engines

Figure 12 depicts the effects of different ammonia injection timings on the cylinder pressure and heat release rate under the condition that the injection interval between diesel and ammonia is fixed at 0.5 °CA. It can be observed from the figure that, with a delay in the ammonia injection timing, the cylinder pressure shows an overall decreasing trend. This phenomenon can be attributed to two main factors: firstly, an earlier ammonia injection time contributes to improving the mixture of diesel and ammonia in the cylinder, thereby promoting a more effective combustion process; secondly, an earlier injection time causes the fuel to start burning and releasing energy before the top dead center, increasing the rate of pressure rise, and consequently leading to an increase in cylinder pressure.

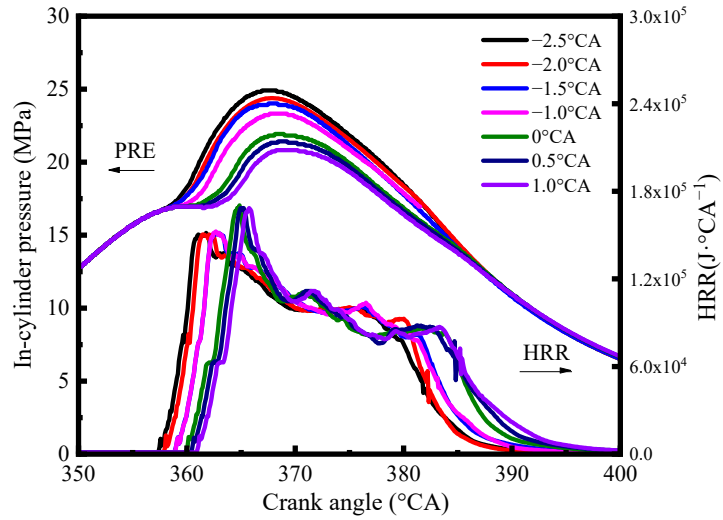

Figure 12. Effect of injection timing on in-cylinder pressure and heat release rate.

Figure 13 illustrates the variation in engine combustion characteristics under different ammonia injection timings. Upon observing the results, it is evident that with the delay in injection timing before reaching the top dead center (TDC), both the start of combustion and the center of the heat release shift towards later crankshaft angles. One reason for this change is that the delayed injection timing leads to a delayed mixing of combustion gases with air, thus delaying the start of combustion accordingly. Another reason is that the combustion propagation slows down due to the delayed injection timing, causing the center of the heat release to move backwards and prolonging the combustion duration.

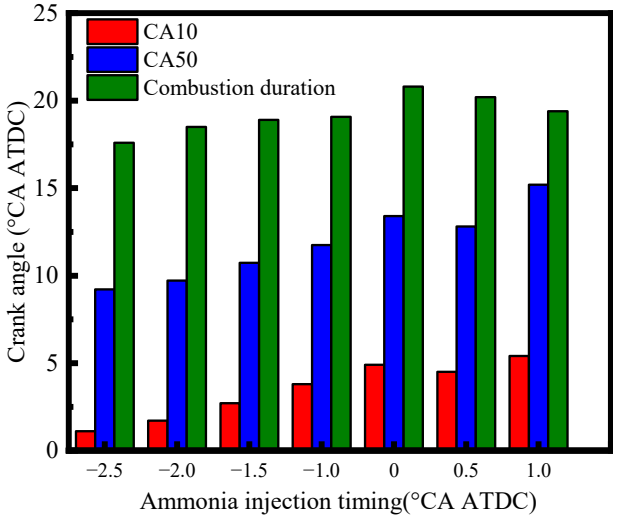

Figure 13. Comparison of CA10, CA50 and combustion duration with different injection timings.

When the injection timing occurs after the top dead center, there is a significant backward shift in both the start of combustion and the center of the heat release, while the combustion duration decreases. This phenomenon is attributed to the fact that combustion mainly occurs during the piston's downward stroke, during which cylinder temperatures and pressures are higher, facilitating accelerated combustion.

Figure 14 depicts the effects of different ammonia injection timings on the engine's mean effective pressure, the indicated thermal efficiency and the indicated specific fuel consumption. The analysis results reveal that, as the ammonia injection time is delayed, both the IMEP and ITE exhibit fluctuations but show an overall decreasing trend. Before the ammonia injection time approaches the TDC, the decrease in IMEP and ITE is relatively slow.

After reaching the top dead center, there is a significant decrease in both the mean effective pressure and the indicated thermal efficiency. Meanwhile, the trend of the indicated specific fuel consumption (ISFC) is opposite to that of the mean effective pressure and the indicated thermal efficiency. As the ammonia injection time is delayed, the ISFC gradually increases, especially when the ammonia injection time reaches the top dead center, there is a significant rise in the ISFC, followed by a stabilization. The main reasons for this change include: the delayed ammonia injection time leads to insufficient time for thorough mixing and atomization of ignition fuel and ammonia fuel, thereby reducing combustion efficiency, and resulting in a decrease in the mean effective pressure and the indicated thermal efficiency; simultaneously, at the start of combustion, the piston is positioned lower, causing a cooling effect on the engine cylinder's components such as the piston and cylinder wall, which leads to partial thermal energy loss, and further affects engine performance. Overall, injecting ammonia before 1 °CA BTDC can essentially achieve the original engine combustion performance.

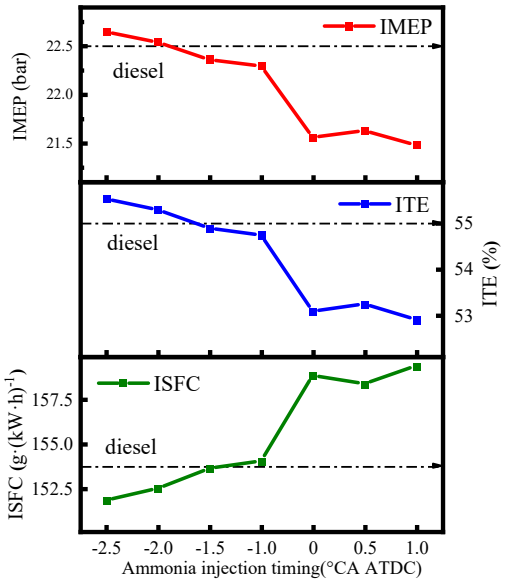

Figure 14. Comparative analysis of IMEP, ITE and ISFC across various injection timings.

Combining Figure 15a,b, it can be observed that as the ammonia injection timing is delayed, the area of high temperature (deep-red) decreases. This phenomenon may be attributed to the early mixing of ammonia with air before reaching the top dead center, leading to the commencement of the combustion process before the piston reaches the top dead center, resulting in rapid heat accumulation and a localized temperature rise. In contrast, in conditions after the top dead center, the combustion process occurs later, and the piston has already begun to descend, resulting in a decrease in the area of high temperature.

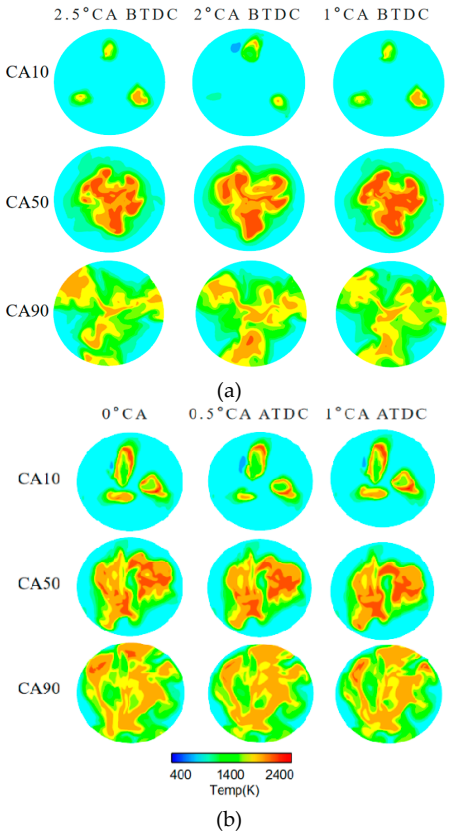

Figure 15. Effect of in-cylinder temperature distribution on (**a**) ammonia injection timing before TDC and (**b**) ammonia injection timing after TDC.

Considering the significant differences in the combustion characteristics of ammonia compared to traditional fossil fuels, and the disparities in spatial scale and operational status between low-speed and medium/high-speed marine engines, this section continues the investigation on the impact of different ammonia injection timings on the combustion and emission characteristics of low-speed engines based on Section 3.1. The aim is to determine the optimal injection timings.

Under the conditions of a 100% load, a 95% ammonia energy substitution rate, and an injection pressure of 700 bar, with diesel injection advanced by 0.5 °CA, simulations were conducted at ammonia injection timings of 2.5, 2.0, 1.5, 1 °CA BTDC, 0, 0.5, and 1 °CA ATDC.

Figure 16 illustrates the variations in major emissions of the engine under different ammonia injection timings. It can be observed from the graph that with the delay in the ammonia injection time, there is an overall reduction in NO_X emissions. Particularly, under these conditions and before reaching the top dead center (TDC), the NO_X emissions decrease with the delay in the ammonia injection time. This reduction may be attributed to the synchronization of the ammonia injection time with the high-temperature zone in the combustion chamber near the TDC, which helps in reducing the area of the local high-temperature and effectively inhibits NO_X formation.

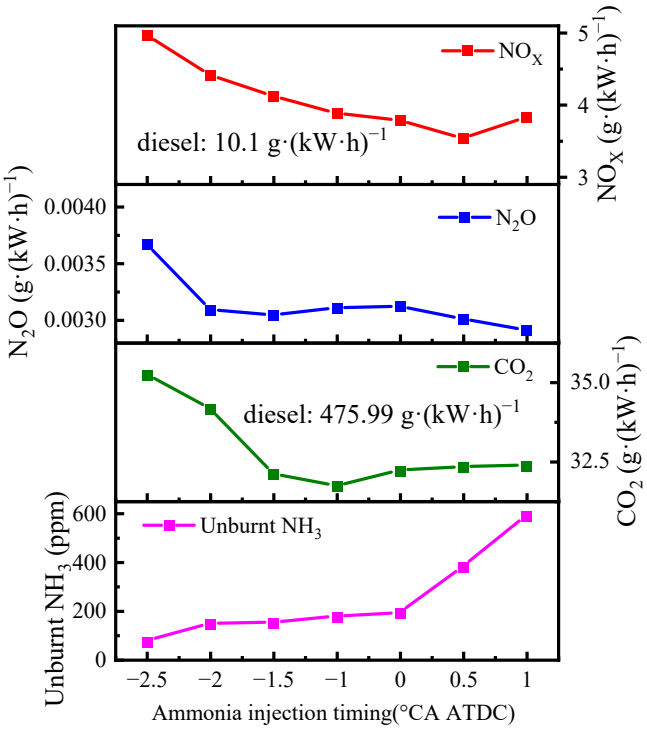

Figure 16. Comparison of NO_X, N_2O, CO_2 and unburnt NH_3 at different injection timings.

The trends in N_2O and CO_2 emissions are similar to NO_X, showing a decrease overall under conditions before reaching TDC and stabilizing after reaching TDC. This phenomenon is due to the smaller area of the local high-temperature zone before reaching TDC, which reduces the generation of N_2O and CO_2. After reaching TDC, the dissipation of heat in the combustion chamber causes a decrease in cylinder temperature compared to before, slowing down the generation of N_2O and CO_2, and resulting in minor changes in emissions.

The emission of unburnt NH_3 shows a gradual increasing trend, mainly because the reduction in mixing time between ammonia and air leads to decreased uniformity of the mixture, reducing combustion efficiency, and subsequently increasing the emission of unburnt NH_3.

Figure 17 depicts the distribution of NO_X in the cylinder under different ammonia injection timings before and after reaching TDC. It can be observed from the graph that with the delay in the ammonia injection time, the area of the NO_X distribution region gradually decreases, especially the reduction in the area of the high concentration region is more significant. This phenomenon indicates that delaying the ammonia injection time contributes to reducing NO_X generation. The possible reason is that delaying the ammonia injection time reduces the mixing time between ammonia and fuel, resulting in a decrease in the average temperature in the cylinder during the combustion process, and thereby reducing NO_X generation. The distribution of NO_X after reaching TDC shows significant differences compared to before reaching TDC, although there is not much change in the distribution area, which corroborates the analysis in Figure 16.

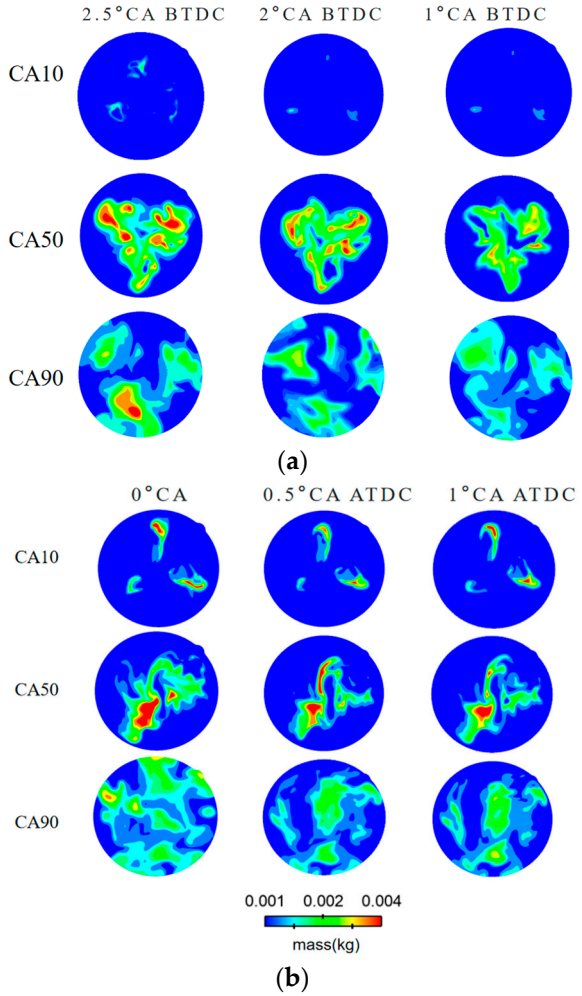

Figure 17. In-cylinder NO_X distribution at different injection timings: (**a**) ammonia injection timing before TDC and (**b**) ammonia injection timing after TDC.

3.3. Effect of Diesel/Ammonia Injection Strategy on Combustion and Emission Characteristics of Low-Speed Engines

Figure 18 illustrates the impacts of different injection strategies on the in-cylinder mean pressure and heat release rate. As depicted in the figures, compared to the D-A (diesel-ammonia) mode, the A-D-A (ammonia-diesel-ammonia) mode significantly increases the initial rate of rise in the in-cylinder pressure, with an earlier and more pronounced peak phase shift. This is primarily due to the pre-injection of ammonia, which evaporates within the cylinder and rapidly forms a combustible mixture, effectively accelerating the combustion rate. Additionally, an increase in the pre-injection proportion further elevates the peak values of the in-cylinder pressure. Moreover, the peak phase of the heat release rate

advances and significantly heightens, with the heat release curve reflecting characteristics of premixed combustion.

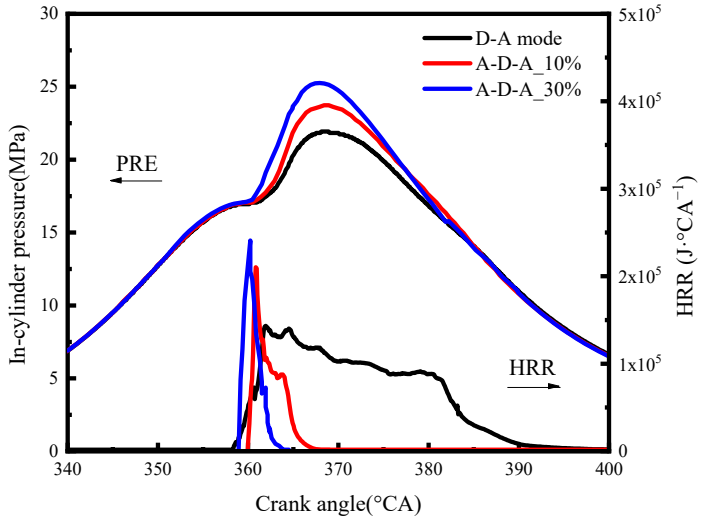

Figure 18. Effect of injection strategy on in-cylinder pressure and heat release rate.

Figure 19 presents a comparison of the CA10, CA50, and combustion duration under different injection strategies. It can be observed that, compared to the D-A mode, the A-D-A mode significantly advances the CA10 and CA50, and also substantially shortens the combustion duration. This is primarily due to the addition of pre-injected ammonia, which initiates combustion earlier and accelerates the reaction rate. Additionally, increasing the pre-injection ammonia ratio from 10% to 30% further advances the CA10 and CA50, and continues to shorten the combustion duration. This is mainly attributed to the increased proportion of pre-injected ammonia, which enhances the fraction of premixed combustion and consequently speeds up the combustion rate.

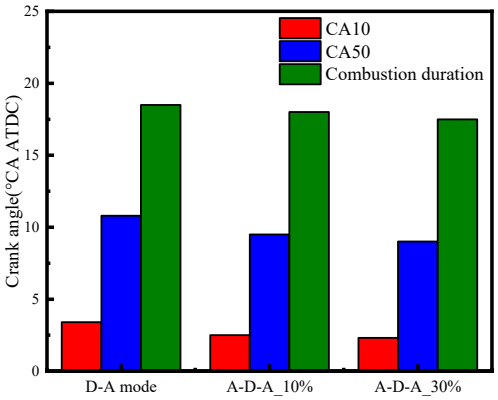

Figure 19. Comparison of CA10, CA50 and combustion duration under different injection strategies.

Figure 20 depicts the comparison of the mean effective pressure, the indicated thermal efficiency, and the indicated specific fuel consumption under various injection strategies. The results demonstrate that the A-D-A mode exhibits higher mean effective pressure and indicated thermal efficiency compared to the baseline engine, while also achieving lower indicated specific fuel consumption. Furthermore, an increase in the pre-injection ammonia ratio further enhances these effects, underscoring the significant role of the A-D-A mode in improving the combustion performance of dual-fuel low-speed engines.

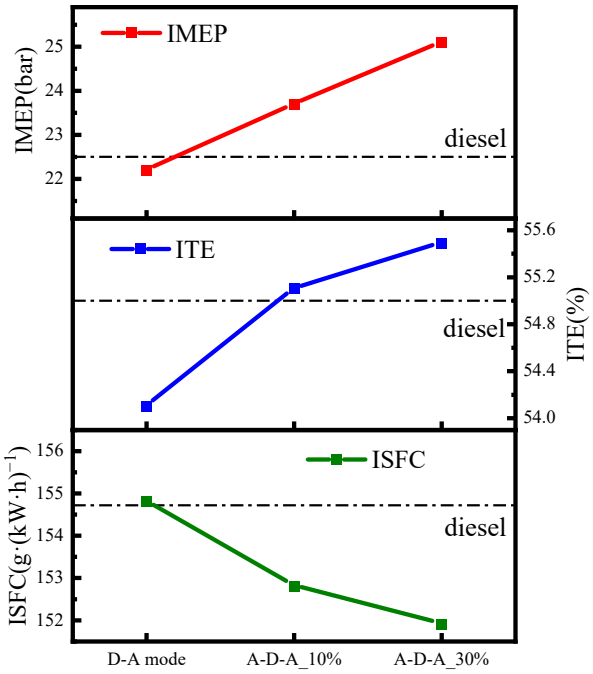

Figure 20. Comparison of IMEP, ITE and ISFC under different injection strategies.

Figure 21 presents a comparison of the in-cylinder average temperature distribution under different injection strategies. It is evident that in the A-D-A mode, the CA10 occurs earlier, and compared to the D-A mode, the temperature distribution at CA50 is more uniform with a larger area of high-temperature regions. Additionally, as the pre-injection ammonia ratio increases, the area of the high-temperature regions within the cylinder also expands. This indicates the effectiveness of the A-D-A mode in achieving a more favorable temperature distribution during combustion.

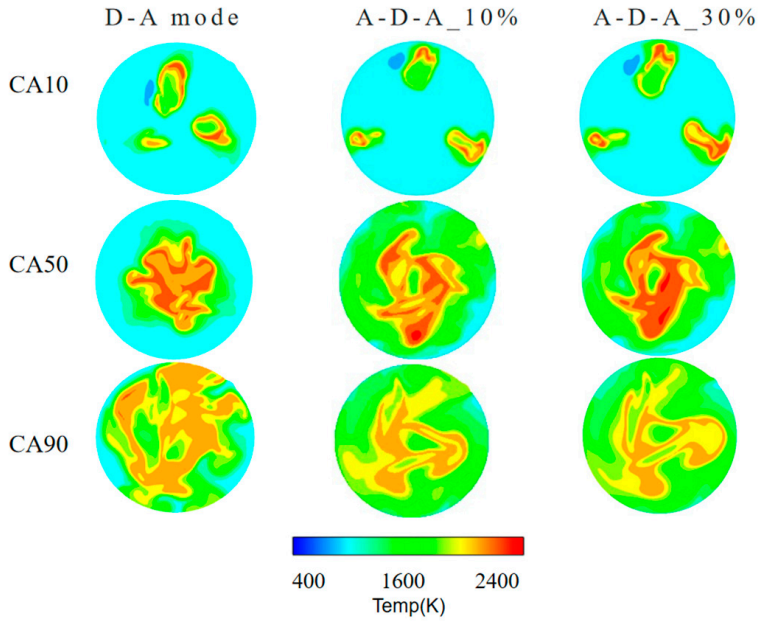

Figure 21. Comparison of average in-cylinder temperature distribution under different injection strategies.

Figure 22 illustrates the comparative emissions of NO_X, N_2O, CO_2 and unburnt NH_3 under various injection strategies. It can be observed that in the A-D-A mode, the emissions of NO_X and CO_2 are significantly elevated, while N_2O emissions decrease and unburnt

NH_3 is substantially reduced. Despite the significant increase in NO_X and CO_2 emissions, their levels remain substantially lower than those of the baseline engine.

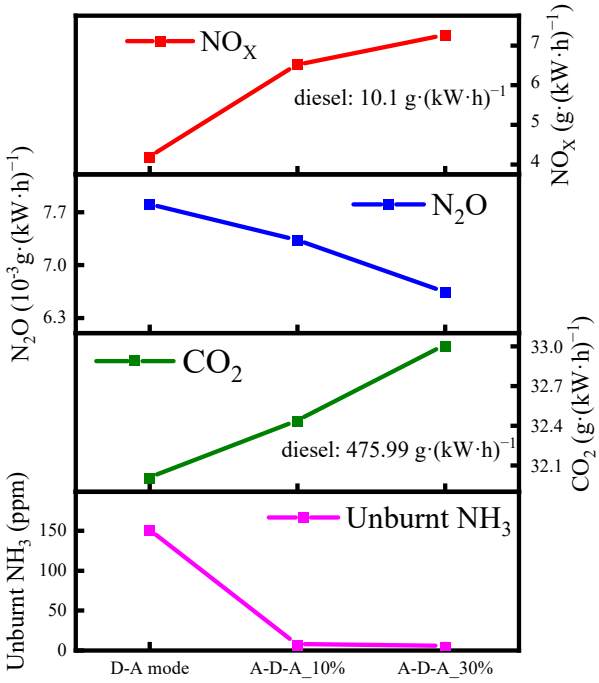

Figure 22. Comparison of NO_X, N_2O, CO_2 and unburnt NH_3 with different injection strategies.

Figure 23 shows a comparison of the in-cylinder NO_X distribution under different injection strategies. The contour plots indicate that the A-D-A mode leads to an increase in NO_X production and an expansion of its distribution area compared to the D-A mode. Additionally, an increase in the pre-injection ammonia ratio further enhances the in-cylinder distribution of NO_X, highlighting the influence of pre-injected ammonia on NO_X formation.

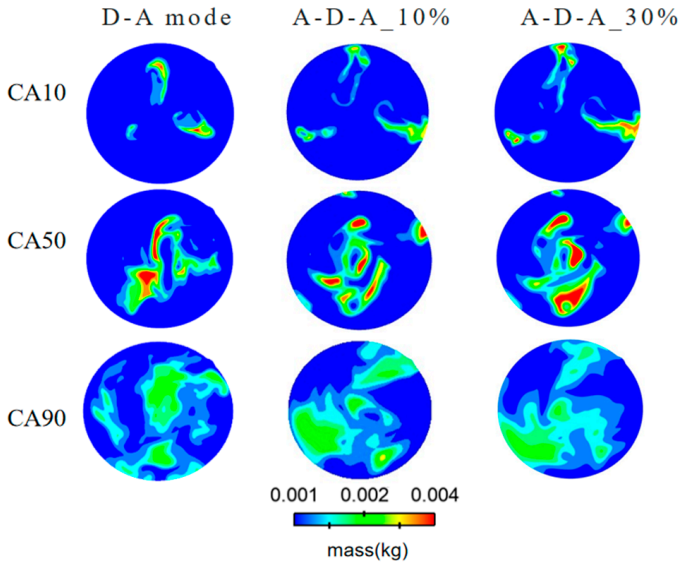

Figure 23. In-cylinder NO_X distribution at different injection strategies.

4. Conclusions

In this study, utilizing a simulation computational model developed for a diesel/ammonia dual-fuel marine low-speed engine, we investigated the impact of various injection strate-

gies on engine combustion and emission characteristics in a dual-fuel mode. The key findings of our research are summarized as follows:

1. The injection pressure of diesel and ammonia significantly influences the combustion and emission characteristics of dual-fuel engines. Appropriately increasing the injection pressure enhances the mean effective pressure and indicated thermal efficiency, thereby reducing the indicated specific fuel consumption. Concerning emissions, the emissions of NO_X and CO_2 are substantially reduced compared to the diesel mode. However, excessively high injection pressures may have a detrimental effect on combustion. Simulation results indicate that at an injection pressure of 700 bar, the combustion performance and emissions can reach a relatively optimal state.
2. The combustion and emission characteristics of dual-fuel low-speed engines are highly sensitive to the timing of ammonia injection. When ammonia is injected 0.5 °CA after diesel injection, as the injection timing is retarded, the mean effective pressure and indicated thermal efficiency gradually decrease, while the indicated specific fuel consumption gradually increases. However, at this point, there is a noticeable decrease in NO_X and N_2O emissions in the exhaust gases. Nevertheless, after reaching the top dead center, the emission of unburnt ammonia increases significantly. Therefore, injecting ammonia before the TDC (approximately 1 °CA BTDC) can effectively reduce emissions to a more favorable level while maintaining engine performance. At this timing, compared to the diesel mode, NO_X emissions decrease by 67.5%, and CO_2 emissions decrease by 93.7%.
3. The impact of different injection strategies on the combustion and emission characteristics of low-speed engines is pronounced. Employing the pre-injection ammonia-diesel-ammonia main injection (A-D-A) mode, while enhancing emission levels, significantly improves the combustion conditions of the low-speed engine. It is recommended to adopt a strategy using 10% pre-injection ammonia, which can increase the mean effective pressure by 1.2 bar compared to the diesel mode and reduce the indicated specific fuel consumption by 0.7 $g\cdot(kW\cdot h)^{-1}$. At the same time, the NO_X emissions have increased by 2.4 $g\cdot(kW\cdot h)^{-1}$, compared to the D-A mode. However, compared to the diesel model, NO_X is still reduced by 35%. Meanwhile, emission standards can be ensured with the help of post-processing equipment.

Author Contributions: Conceptualization, Q.W. and Z.Z.; methodology, Z.Z.; software, Z.Z.; validation, Q.W. and Z.Z.; formal analysis, Q.W.; resources, X.L., T.L. and L.C.; data curation, Q.W.; writing—original draft preparation, Q.W.; writing—review and editing, X.L.; visualization, Q.W.; project administration, X.L, T.L. and L.C.; funding acquisition, X.L. All authors have read and agreed to the published version of the manuscript.

Funding: This research was funded by the National Natural Science Foundation of China (NSFC). Project, grant number 52342606, 51976135, and the China Ministry of Industry and Information Technology High-tech Ship Project.

Data Availability Statement: The original contributions presented in the study are included in the article, further inquiries can be directed to the corresponding author.

Conflicts of Interest: Authors Lei Cui and Teng Liu were employed by the company China Ship Power Institute Co., Ltd. The remaining authors declare that the research was conducted in the absence of any commercial or financial relationships that could be construed as a potential conflict of interest.

References

1. Cardoso, J.S.; Silva, V.; Rocha, R.C.; Hall, M.J.; Costa, M.; Eusébio, D. Ammonia as an Energy Vector: Current and Future Prospects for Low-Carbon Fuel Applications in Internal Combustion Engines. *J. Clean. Prod.* **2021**, *296*, 126562. [CrossRef]
2. Gray, J.T.; Dimitroff, E.; Meckel, N.T.; Quillian, R.D. Ammonia Fuel—Engine Compatibility and Combustion. *SAE Trans.* **1967**, *75*, 785–807.
3. Langella, G.; de Joannon, M.; Sabia, P.; Iodice, P.; Amoresano, A. Ammonia as a Fuel for Internal Combustion Engines: Latest Advances and Future Challenges. *J. Phys. Conf. Ser.* **2022**, *2385*, 012036. [CrossRef]

4. International Maritime Organization. Reduced limit on sulphur in marine fuel oil implemented smoothly through 2020. 2020. Available online: https://www.imo.org/en/MediaCentre/PressBriefings/pages/02-IMO-2020.aspx (accessed on 1 May 2023).
5. Internation Maritime Organization. Prevention of Air Pollution from Ships MARPOL Annex VI Proposal to Initiate a Revision. 2005. Available online: https://www.imo.org/en/about/Conventions/Pages/International-Convention-for-the-Prevention-of-Pollution-from-Ships-(MARPOL).aspx (accessed on 1 May 2023).
6. Shin, J.; Park, S. Numerical Analysis for Optimizing Combustion Strategy in an Ammonia-Diesel Dual-Fuel Engine. *Energy Convers. Manag.* **2023**, *284*, 116980. [CrossRef]
7. Ryu, K.; Zacharakis-Jutz, G.E.; Kong, S.-C. Effects of Gaseous Ammonia Direct Injection on Performance Characteristics of a Spark-Ignition Engine. *Appl. Energy* **2014**, *116*, 206–215. [CrossRef]
8. Pochet, M.; Dias, V.; Moreau, B.; Foucher, F.; Jeanmart, H.; Contino, F. Experimental and Numerical Study, under LTC Conditions, of Ammonia Ignition Delay with and without Hydrogen Addition. *Proc. Combust. Inst.* **2019**, *37*, 621–629. [CrossRef]
9. Nadimi, E.; Przybyła, G.; Lewandowski, M.T.; Adamczyk, W. Effects of Ammonia on Combustion, Emissions, and Performance of the Ammonia/Diesel Dual-Fuel Compression Ignition Engine. *J. Energy Inst.* **2023**, *107*, 101158. [CrossRef]
10. Song, Y.; Marrodán, L. The Sensitizing Effects of NO_2 and NO on Methane Low Temperature Oxidation in a Jet Stirred Reactor. *Proc. Combust. Inst.* **2019**, *37*, 667–675. [CrossRef]
11. Wei, H.; Chen, X.; Wang, G.; Zhou, L.; An, S.; Shu, G. Effect of Swirl Flow on Spray and Combustion Characteristics with Heavy Fuel Oil under Two-Stroke Marine Engine Relevant Conditions. *Appl. Therm. Eng.* **2017**, *124*, 302–314. [CrossRef]
12. Kasper, A.; Aufdenblatten, S.; Forss, A.; Mohr, M.; Burtscher, H. Particulate Emissions from a Low-Speed Marine Diesel Engine. *Aerosol Sci. Technol.* **2007**, *41*, 24–32. [CrossRef]
13. Bian, J.; Vandooren, J.; Van Tiggelen, P.J. Experimental Study of the Structure of an Ammonia-Oxygen Flame. *Symp. Int. Combust.* **1988**, *21*, 953–963. [CrossRef]
14. Zhou, X.; Li, T.; Wang, N. Pilot Diesel-Ignited Ammonia Dual Fuel Low-Speed Marine Engines: A Comparative Analysis of Ammonia Premixed and High-Pressure Spray Combustion Modes with CFD Simulation. *Renew. Sustain. Energy Rev.* **2023**, *173*, 113108. [CrossRef]
15. Jin, S.; Wu, B.; Zi, Z.; Yang, P.; Shi, T.; Zhang, J. Effects of Fuel Injection Strategy and Ammonia Energy Ratio on Combustion and Emissions of Ammonia-Diesel Dual-Fuel Engine. *Fuel* **2023**, *341*, 127668. [CrossRef]
16. Yousefi, A.; Guo, H.; Dev, S.; Liko, B.; Lafrance, S. Effects of Ammonia Energy Fraction and Diesel Injection Timing on Combustion and Emissions of an Ammonia/Diesel Dual-Fuel Engine. *Fuel* **2022**, *314*, 122723. [CrossRef]
17. Lu, Z.; Liu, M.; Shi, L.; Wang, T.; Lu, T.; Wang, H. Numerical Research of the Injected Exhaust Gas Recirculation Strategy on a Two-Stroke Low-Speed Marine Diesel Engine. *Energy* **2022**, *244*, 122731. [CrossRef]
18. Zhang, Z.; Long, W.; Dong, P.; Tian, H.; Tian, J.; Li, B.; Wang, Y. Performance Characteristics of a Two-Stroke Low Speed Engine Applying Ammonia/Diesel Dual Direct Injection Strategy. *Fuel* **2023**, *332*, 126086. [CrossRef]
19. Liu, H.; Li, J.; Wang, J.; Wu, C.; Liu, B.; Dong, J.; Liu, T.; Ye, Y.; Wang, H.; Yao, M. Effects of Injection Strategies on Low-Speed Marine Engines Using the Dual Fuel of High-Pressure Direct-Injection Natural Gas and Diesel. *Energy Sci. Eng.* **2019**, *7*, 1994–2010. [CrossRef]
20. Gross, C.W.; Kong, S.-C. Performance Characteristics of a Compression-Ignition Engine Using Direct-Injection Ammonia–DME Mixtures. *Fuel* **2013**, *103*, 1069–1079. [CrossRef]
21. Reiter, A.J.; Kong, S.-C. Combustion and Emissions Characteristics of Compression-Ignition Engine Using Dual Ammonia-Diesel Fuel. *Fuel* **2011**, *90*, 87–97. [CrossRef]
22. Niki, Y.; Nitta, Y.; Sekiguchi, H.; Hirata, K. Diesel Fuel Multiple Injection Effects on Emission Characteristics of Diesel Engine Mixed Ammonia Gas Into Intake Air. *J. Eng. Gas Turbines Power* **2019**, *141*, 061020. [CrossRef]
23. Cui, L.; Wang, H. Numerical Simulation Study of In-Cylinder Combustion in Marine Ammonia-Fuelled Low-Speed Engine. In Proceedings of the 2022 Annual Conference on Combustion of Chinese Society of Engineering Thermophysics, Shanghai, China, 16 December 2022; Volume 224215.
24. Cui, L.; Wang, H. Simulation Research on the Combustion of Marine Low-Speed Ammonia Engine. *J. Eng. Thermophys.* **2023**, *44*, 3151–3159.

Disclaimer/Publisher's Note: The statements, opinions and data contained in all publications are solely those of the individual author(s) and contributor(s) and not of MDPI and/or the editor(s). MDPI and/or the editor(s) disclaim responsibility for any injury to people or property resulting from any ideas, methods, instructions or products referred to in the content.